2010 International Symposium on Nonlinear Theory and its Applications
NOLTA2010, Krakow, Poland, September 5-8, 2010

Application of Particle Swarm Optimizers to Finding Desired Parameters of Switched Dynamical Systems

Haruna Matsushita† and Toshimichi Saito†

†Dept. of Electrical and Electronics Engineering, Hosei University
3–7–2 Kajino-cho, Koganei, Tokyo 184–8584, Japan

Abstract—This paper studies a novel application of particle swarm optimizers to finding desired parameters for multi-objective problems in switched dynamical systems. We consider a simplified model of photovoltaic systems such that the input is a single solar cell and is converted to the output via a boost converter. We define realizable parameters with large average power as a desired parameter set. From simulation results, the efficiency of the proposed algorithm is confirmed.

1. Introduction

The Particle Swarm Optimization (PSO) [1]–[2] is an algorithm to simulate the movement of flocks of birds. Each particle of swarm tries to find a better solution according to its personal best position and the swarm best position. The many real/potential applications have been proposed, including design of artificial neural networks, digital filters, power systems and power converters [3]–[6]. It should be noted that the PSO does not require differentiability of the objective function that is a compulsory item in the gradient methods. The PSO is well suited for application to circuits with discontinuous switching that are widely used in a variety of switching power converters.

This paper proposes an application of the PSO to analysis of switched dynamical systems (SDS). The SDS can exhibit rich bifurcation phenomena [7]–[8] and relates to many engineering systems including power converters. In this study, we consider an example of the SDS which is a simplified model of photovoltaic (PV) systems such that the input is a single solar cell and is converted to the output via a boost converter [9]. Since the maximum power point (MPP) of the PV system depends on the operating terminal voltage and current, the maximum power point tracker has been studied as a key technique [10]-[11]. Our SDS includes the solar cell input modeled by a current-controlled voltage source (CCVS) having piecewise linear (PWL) characteristics that can be regarded as a simplified version of the existing smooth model [12]. A switching rule is a variant of peak-current-controlled switching and can cause various bifurcation phenomena. It has been investigated that as a parameter varies, a stable periodic orbit (SPO) is changed into an unstable periodic orbit (UPO) via period-doubling bifurcation and another SPO appears. Furthermore, the UPO can have larger average power than the SPO and can have the MPP.

This paper proposes an application of the PSO to multi-objective problems (MOP) and applies the proposed algorithm to find desired parameters for the MOP in the SDS. The MOP is described by the hybrid fitness functions consisting of the functions evaluating the validity of parameters and criteria. We define a parameter, which is a period-doubling bifurcation set and is the MPP, as a desired parameter which is realizable with large average power. From simulation results, we confirm that the PSO for the MOP can easily find the desired parameter although a numerical calculation needs huge calculation amount.

2. Particle Swarm Optimizer for Multi-objective problems

We propose the application of the PSO to the MOP.

Let us consider a positive definite multi-objective function of parameters $\vec{a} \equiv (a_1, a_2, \cdots, a_D)$;

$$F_j(\vec{a}) \geq 0,\ j = 1, 2, \cdots, M, \tag{1}$$

where $M = 1$ and $M \geq 2$ correspond to an uni-objective problem and a MOP, respectively. Although usual optimization algorithms try to find the minimum value of F_j, we introduce the inequalities

$$0 \leq F_j(\vec{a}) < C_j, \tag{2}$$

where C_j is the j-th criterion. Our problem is finding parameter values that satisfy Eq. (2). This flexibility can help to search a suitable solution and can give better result than MOP without the criterion.

In the algorithm of PSO, multiple potential solutions called "particles" coexist. Each particle has two informations; position and velocity. The position vector of i-th particle at discrete time n and its velocity vector are represented by $\vec{a}_i(n) \equiv (a_{i1}, a_{i2}, \cdots, a_{iD}) \in \Re^D$ and $\vec{v}_i(n) \equiv (v_{i1}, v_{i2}, \cdots, v_{iD}) \in \Re^D$, respectively, where ($i = 1, 2, \cdots, N$). The position corresponds to the parameter $\vec{a}$ in Eq. (2). Each particle moves toward the personal best position $\vec{a}_{p_i}$ ($pbest_i$), which is the past best position of i-th particle, and the global best position $\vec{a}_g$ ($gbest$) which is the best $pbest$ among all the particles. The $\vec{a}_g$ is the potential solution at time n.

Step 1 (Initialization): Let a discrete generation step $n = 0$. Randomly initialize the particle position $\vec{a}_i(n)$ in the search

space $Ds \subset \Re^D$, and initialize other variables; velocity $\vec{v}_i(n) = 0$, $\vec{a}_{p_i} = \vec{a}_i(n)$ and $\vec{a}_g = \vec{a}_1(n)$.
Step 2 (Evaluation): Terminate the algorithm if

$$0 \le F_j(\vec{a}_g) < C_j \ \text{ for } \ j = 1, 2, \cdots, M. \tag{3}$$

If not, go to Step 3.
Step 3 (Updating): Update $\vec{v}_i$ and $\vec{a}_i$ of each particle i;

$$\begin{aligned} &\vec{v}_i(n+1) \\ &\quad = w\vec{v}_i(n) + \vec{r}_1\rho_1(\vec{a}_{p_i} - \vec{a}_i(n)) + \vec{r}_2\rho_2(\vec{a}_g - \vec{a}_i(n)), \\ &\vec{a}_i(n+1) = \vec{a}_i(n) + \vec{v}_i(n+1), \end{aligned} \tag{4}$$

where w is the inertia weight determining how much of the previous velocity of the particle is preserved. $\vec{r}_1$ and $\vec{r}_2$ are D-dimensional uniform random number vectors from U(0,1). ρ_1 and ρ_2 are two positive acceleration coefficients.
Step 4 (Hybrid fitness): Renew $pbest_i$ if the fitness is improved or satisfies the criteria. Let $\vec{a}_{p_i} = \vec{a}_i(n+1)$ if

$$F_j(\vec{a}_i(n+1)) < F_j(\vec{a}_{p_i}) \text{ OR } F_j(\vec{a}_i(n+1)) < C_j, \tag{5}$$

is satisfied for all the objective functions. Renew $gbest$ as $\vec{a}_g = \vec{a}_{p_i}$, where i is a particle whose $pbest_i$ satisfies

$$F_j(\vec{a}_{p_i}) < F_j(\vec{a}_g) \text{ OR } F_j(\vec{a}_{p_i}) < C_j, \tag{6}$$

for all the objective functions. If more than one particle satisfies Eq. (6), the particle i with the smallest index is chosen.
Step 5 Let $n = n + 1$, return to Step 2 and repeat until the maximum time limit $n_{\max}$.

3. Multi-Objective Optimization for Circuit model of the boost converter with a solar cell.

3.1. Circuit model

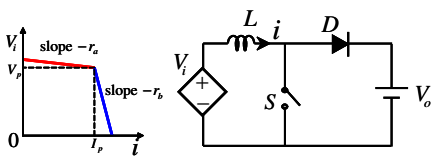

Figure 1: Circuit model of the boost converter with a solar cell

In order to evaluate the performance of the proposed algorithm, we consider detection of the MPP of the SDS which is the simplified model of the PV systems. Figure 1 shows the SDS where the 2-segment PWL CCVS models the solar cell input [9]. The dimensionless circuit equation is described by

$$\frac{dx}{d\tau} = \begin{cases} \gamma y(x), & \text{for State 1} \\ \gamma(y(x) - q), & \text{for State 2,} \end{cases} \tag{7}$$

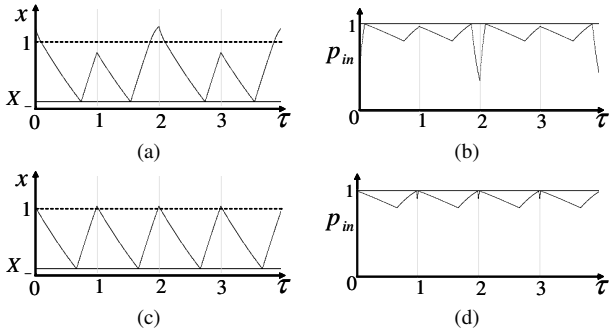

Figure 2: Typical orbits and instantaneous power p_{in} (average power P_A) for $\alpha = 0.5$, $\beta = 9.0$, $q = 1.6$, $X_- = 0.7$ and $\gamma = 0.884$. (a) SPO with period 2 and (b) p_{in} of SPO ($P_A = 0.87$). (c) UPO with period 1 and (d) p_{in} of UPO ($P_A = 0.91$).

$$y(x) = \begin{cases} -\beta(x-1) + 1, & \text{for } x > 1 \\ -\alpha(x-1) + 1, & \text{for } x \le 1, \end{cases} \tag{8}$$

$$\text{SW Rule:} \begin{array}{l} \text{State 2} \to \text{State 1: when } x = X_- > 0. \\ \text{State 1} \to \text{State 2: at } \tau = n \text{ and } x > X_-, \end{array} \tag{9}$$

where the SW rule is a variant to peak-current control. The dimensionless variables and parameters are defined by

$$\begin{aligned} &\tau = \frac{t}{T},\ x = \frac{i}{I_p},\ y(x) = \frac{V_i(I_p x)}{V_p},\ \alpha = \frac{r_a I_p}{V_p} \\ &\beta = \frac{r_b I_p}{V_p},\ q = \frac{V_o}{V_p},\ \gamma = \frac{TV_p}{LI_p},\ X_- = \frac{J_-}{I_p}. \end{aligned} \tag{10}$$

The dimensionless 5 parameters can be classified into two categories: (α, β, q), which characterizes "solar cell and load", and (γ, X_-) which characterizes "switching control". The piece-wise exact solution is given by

$$\begin{aligned} &\text{State 1:} \\ &x(\tau) = (x_0 - x_{e1})e^{-\gamma\alpha(\tau-\tau_0)} + x_{e1}, \quad \text{for } x \le 1 \\ &x(\tau) = (x_0 - x_{e2})e^{-\gamma\beta(\tau-\tau_0)} + x_{e2}, \quad \text{for } x > 1 \\ &\text{State 2:} \\ &x(\tau) = (x_0 - x_{e3})e^{-\gamma\alpha(\tau-\tau_0)} + x_{e3}, \quad \text{for } x \le 1 \\ &x(\tau) = (x_0 - x_{e4})e^{-\gamma\beta(\tau-\tau_0)} + x_{e4}, \quad \text{for } x > 1 \end{aligned} \tag{11}$$

where (τ_0, x_0) denotes an initial condition, $x_{e1} = 1 + 1/\alpha$, $x_{e2} = 1 + 1/\beta$, $x_{e3} = q/\alpha - 1 - 1/\alpha$ and $x_{e4} = q/\beta - 1 - 1/\beta$. Using Eq. (11), we can calculate waveforms precisely. Figures 2(a) and (c) show typical examples; the SPO with period 2 and the UPO with period 1 for the same parameter values as the SPO.

In order to consider the power characteristics, we define the dimensionless instantaneous and average powers;

$$p_{in}(\tau) = \frac{i(t)}{I_p}\frac{V_i(t)}{V_p},\ P_A = \frac{1}{N_p}\int_0^{N_p} p_{in}(\tau)d\tau \tag{12}$$

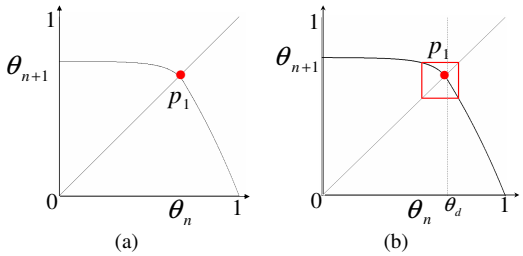

Figure 3: Typical phase maps. $\alpha = 0.5$, $\beta = 0.9$, $q = 1.6$ and $X_- = 0.7$. (a) Stable fixed point p_1 for $\gamma = 1.0$. (b) Stable 2-periodic points for $\gamma = 0.884$. p_1 is unstable.

where $N_p = T_p/T$ is the dimensionless period of the SPO or the UPO for dimensionless time τ. Figures 2(b) and (d) show the instantaneous power $p_{in}(\tau)$ corresponding to Figs. 2(a) and (c), respectively. The UPO as Fig. 2(d) has lower peak, the p_{in} has shallower valley and the P_A is larger than that of the SPO in Fig. 2(b). Although the UPO is not observable, it has larger power than the SPO for the same parameter. Such a UPO can have the MPP for the parameter γ.

In order to analyze and power characteristics, we derive the phase map. Let τ_n denotes the n-th switching time at the lower threshold X_-, and let θ_d be a border time such that a trajectory started from (θ_d, X_-) reaches (1,1). We can describe a one-dimensional map explicitly;

$$F(\tau_n) = \begin{cases} f_1(f_2(f_3(f_4(\tau_n)))), & \text{for } 0 \le \tau_n < \theta_d \\ g_1(g_2(\tau_n)), & \text{for } \theta_d \le \tau_n < 1 \end{cases} \quad (13)$$

where

$$\tau_{n+1} = f_1(\tau_{s2}),\ \tau_{s2} = f_2(x_{s1}),\ x_{s1} = f_3(\tau_{s1}),\ \tau_{s1} = f_4(\tau_n)$$
$$\tau_{n+1} = g_1(x_{s2}),\ x_{s2} = g_2(\tau_n),\ g_2(\theta_d) = 1.$$

Let a phase variable $\theta_n = \tau_n \bmod 1$. The phase map f from the unit interval $I \equiv [0, 1)$ to itself;

$$\theta_{n+1} = f(\theta_n) \equiv F(\theta_n) \bmod 1, \text{ for } \theta_n \in I. \quad (14)$$

As shown in Fig. 3, this phase map forms a convex curve. A point p is said to be a k-periodic point if $p = f^k(p)$ and $p \neq f^l(p)$ for $1 \le l < k$ where $f^l(x_p) = f(f^{l-1}(p))$ and $f^0(p) \equiv p$. A 1-periodic point is referred to as a fixed point. A periodic point p is said to be unstable and stable for initial value if $|Df^k(p)| > 1$ and $|Df^k(p)| < 1$, respectively, where $Df^k(p)$ is the slope of f^k at p. The stable and unstable periodic points correspond to the SPO and UPO of the SDS, respectively.

Figure 4 shows the average power P_A of a fundamental periodic orbit (FPO) which corresponds to the fixed point p_1 in Fig. 3. As γ reaches the first period doubling bifurcation set D_1 and decreases, the FPO is changed from SPO to UPO and the P_A has the peak (i.e., MPP) at $\gamma = 0.884$, namely the MPP for γ ($\partial P_A/\partial\gamma = 0$). The M is one-to-one on the γ versus X_- plane and gives the ridge of the P_A characteristics shown as Fig. 5.

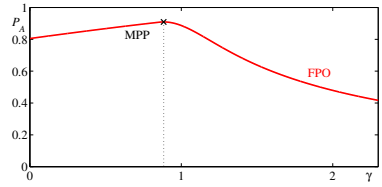

Figure 4: Average power characteristics for $\alpha = 0.5$, $\beta = 9.0$, $q = 1.6$ and $X_- = 0.7$. FPO shows characteristics of the stable/unstable FPO. The maximum average power $P_A = 0.909$ is obtained when $\gamma = 0.884$.

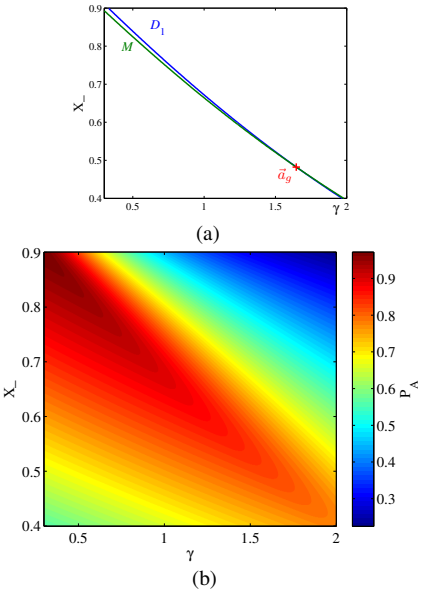

Figure 5: Parameter sets of bifurcation and MPP for $\alpha = 0.5$, $\beta = 0.9$ and $q = 1.6$. (a) D_1: the period doubling bifurcation set. M: ridge of the average power of FPO. (b) The average power P_A corresponding to each parameter set.

3.2. Multi-Objective function

We define multi-objective functions for finding desired parameter set with MPP of the SDS. Since bifurcation analysis in the 5-dimensional parameter space corresponding to particle position $\vec{a}_i$ in the PSO is extremely hard, we focus on 2-dimensional parameters $\vec{a} \equiv (a_1, a_2) \equiv (\gamma, X_-)$ which control the switching. The search space Ds is defined as $0 < a_1 \le 2$ and $0.3 < a_2 \le 0.9$. For convenience, we consider the cross-point of the parameter set M (the MPP for γ) and the period doubling bifurcation set D_1 as the target parameter of the PSO; it is a border of stability of the FPO with MPP for γ. Note that P_A increases as γ decreases and as X_- increases. However, since γ depends on the clock period T and device speed as Eq. (10), the circuit with small γ is unrealizable.

We then define two objective functions. The first one is

about the MPP for γ. Whether $\vec{a}$ is the MPP is obtained by calculating of the slope on present position as

$$F_1(\vec{a}) = \left|\frac{\partial P_A(\vec{a})}{\partial \gamma}\right| = \left|\frac{\partial P_A(\vec{a})}{\partial a_1}\right|. \quad (15)$$

$F_1(\vec{a}) = 0$ means that $\vec{a}$ generates the maximum average power on γ, namely a_1. The second objective function evaluates whether $\vec{a}$ is the period doubling bifurcation set according to

$$F_2(\vec{a}) = |Df(p_1)| - 1. \quad (16)$$

$F_2(\vec{a}) = 0$ means that $\vec{a}$ is the period doubling bifurcation set D_1 shown in Fig. 5, in other words, the system with $\vec{a}$ supplies larger power than that of the SPO. If we can minimize both F_1 and F_2, we can obtain the realizable output having desired power.

By substituting F_1 and F_2 into Eqs. (5) and (6) in Step 4, the proposed algorithm is available for the SDS. Then, the renewal condition of $pbest_i$ and $gbest$ is described by

$$\begin{aligned} &\vec{a}_{p_i} = \vec{a}_i(n+1) \text{ if} \\ &\Big(F_1(\vec{a}_i(n+1)) < F_1(\vec{a}_{p_i}) \text{ OR } F_1(\vec{a}_i(n+1)) < C_1\Big), \\ &\text{AND} \\ &\Big(F_2(\vec{a}_i(n+1)) < F_2(\vec{a}_{p_i}) \text{ OR } F_2(\vec{a}_i(n+1)) < C_2\Big), \end{aligned} \quad (17)$$

$$\begin{aligned} &\vec{a}_g = \vec{a}_{p_i} \text{ if} \\ &\Big(F_1(\vec{a}_{p_i}) < F_1(\vec{a}_g) \text{ OR } F_1(\vec{a}_{p_i}) < C_1\Big), \\ &\text{AND} \\ &\Big(F_2(\vec{a}_{p_i}) < F_2(\vec{a}_g) \text{ OR } F_2(\vec{a}_{p_i}) < C_2\Big). \end{aligned} \quad (18)$$

Note again that if more than one particle satisfies Eq. (18), the particle i with the smallest index is chosen. The terminating condition Eq. (3) is given by

$$F_1(\vec{a}_g) < C_1 \text{ AND } F_2(\vec{a}_g) < C_2, \quad (19)$$

4. Numerical experiments

For numerical experiments, we use the following parameters;

$$N = 30,\ w = 0.7,\ \rho_1 = \rho_2 = 1.5,\ n_{\max} = 1500.$$
$$C_1 = 2.5e^{-4},\ C_2 = 5.0e^{-4}.$$

Figure 6 shows typical changes of the average power P_A of $gbest$ and typical fitness functions in the searching process. The obtained result is the average power $P_A = 0.8182$ with $\gamma = 1.6463$ and $X_- = 0.4823$. From Fig. 6(b), we can observe that the two fitness functions converged on the criterion C_1 and C_2, not only decreasing, but also increasing. This effect was caused by the two criterion in Eqs. (17) and (18). Each decrease of the two fitness helps other increase, and this effect leads the P_A to the maximum average power with the realizable parameters. Figure 5 shows the parameter $\vec{a}_g$ obtained by the simulation. From this figure, we can say that the proposed algorithm has found the intersection of M and D_1, namely the desired parameter.

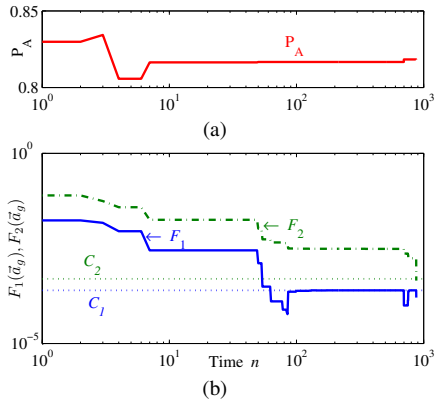

Figure 6: Search process for $\alpha = 0.5$, $\beta = 0.9$ and $q = 1.6$. (a) Change of the average power of $gbest$. (b) Search process of $F_1(\vec{a}_g)$ and $F_2(\vec{a}_g)$. F_1 and F_2 reached C_1 and C_2 at $n = 63$ and 875, respectively.

5. Conclusions

This study has proposed the application of the PSO to finding the desired parameters of the SDS. In order to find the desired parameters, we have defined the MOP which evaluates the average power of the system and whether the parameters are realizable. Performing basic numerical experiments, we have confirmed the algorithm efficiency.

References

[1] A. P. Engelbrecht, Fundamentals of computational swarm intelligence, Willey, 2005.

[2] E. Miyagawa and T. Saito, Particle swarm optimizers with growing tree topology. IEICE Trans. Fundamentals, E92-A, pp. pp. 2275-2282, 2009.

[3] Garro, B. A., Sossa, H., Vazquez, R. A.: Design of artificial neural networks using a modified particle swarm optimization algorithm, in Proc. IEEE-INNS Int'l Joint Conf. Neural Netw., pp. 938-945, 2009.

[4] F. Teixeira and A. Romariz, Digital filter arbitrary magnitude and phase approximations-statistical analysis applied to a stochastic-based optimization approach, in Proc. Congr. Evol. Comput., pp. 4089-4096, 2008.

[5] Y. Valle, G. K. Venayagamoorthy, S. Mohagheghi J.-C. Hernandez and R. G. Harley, Particle swarm optimization: basic concepts, variants and applications in power systems, IEEE Trans. Evol. Comput., 12, 2, pp. 171-195, 2008.

[6] K. Ono and T. Saito, Application of Particle Swarm Optimizers to Two-Objective Problems in Design of Switching Inverters, in Proc. IEEE-INNS Int'l Joint Conf. Neural Netw., pp. 2353-2357, 2009.

[7] S. Banerjee and G. C. Verghese, eds., Nonlinear Phenomena in Power Electronics: Attractors, Bifurcations, Chaos, and Nonlinear Control, IEEE Press, 2001.

[8] C. K. Tse and M. di Bernardo, Complex behavior in switching power converters, Proc. IEEE, 90, pp. 768-781, 2002.

[9] D. Kimura and T. Saito, A Simple Switched Dynamical System based on Photovoltaic Systems, Proc. of NOLTA, pp. 487-490, 2009.

[10] M. Veerachary, T. Senjyu and K. Uezato, Neural-Network-Based Maximum-Power-Point Tracking of Coupled-Inductor Interleaved-Boost-Converter-Supplied PV System Using Fuzzy Controller, IEEE Trans. Ind. Electron., 50, 4, pp. 749-758, 2003.

[11] D. Sera, R. Teodorescu, J. Hantschel and M. Knoll, Optimized Maximum Power Point Tracker for Fast-Changing Environmental Conditions, IEEE Trans. Ind. Electron., 55, 7, pp. 2629-2637, 2008.

[12] P. Maffezzoni and Dario D' Amore, Compact Electrothermal Macromodeling of Photovoltaic Modules, IEEE Trans. Circuits Syst. II, 56, 2, pp. 2009.